Multiply Twinned Morphologies of FePt and CoPt Nanoparticles

Markus E. Gruner, Georg Rollmann, Peter Entel, and Michael Farle

Physics Department and Center for Nanointegration CENIDE, University of Duisburg-Essen, 47048 Duisburg, Germany

(Received 30 July 2007; published 28 February 2008)

Based on large-scale density functional theory calculations we provide a systematic overview of the size dependence of the energetic order and magnetic properties of various morphologies of FePt and CoPt clusters with diameters of up to 2.5 nm. For FePt, ordered multiply twinned icosahedra and decahedra are more favorable than the $L1_0$ phase throughout the investigated size range. For CoPt, segregated morphologies predominate with considerably increased energy differences to the $L1_0$ structure. The compositional trends are traced back to differences between the morphologies in the partial electronic density of states associated with the $3d$ element.

DOI: 10.1103/PhysRevLett.100.087203 PACS numbers: 75.75.+a, 36.40.Mr, 61.46.Df, 75.50.Ss

The physics of small transition-metal nanoparticles has attracted much attention from a fundamental science point of view [1–3]. In the size range of several hundreds to a few thousands of atoms, a critical ratio of surface and volume atoms is reached, where structural crossover phenomena [4,5] and electronic confinement effects are observed. The close interrelation of electronic structure and morphology requires a quantum-mechanical description in the framework of density functional theory (DFT) combining the necessary accuracy while providing the scalability to the interesting system sizes on contemporary supercomputers (e.g., [2,6]). Less expensive approaches relying on empirical potentials permit extensive finite temperature and dynamical studies but request a careful calibration of parameters to experimental and theoretical data in order to describe the specific structural environments appropriately. In experiment, significant progress has been made in driving the resolution of transmission electron microscopy (HRTEM) down to the sub-Å limit [7,8] permitting the direct observation of clusters in the nanometer range [9]. In this way, morphologies, layer resolved surface relaxation [10], and changes after thermal treatments can be identified, while large-scale DFT calculations provide ground state properties as total energies, magnetic moments, and electronic density of states (DOS). Approaching realistic diameters for future storage applications, the present work provides for the first time a systematic investigation of size dependence, energetic order, and magnetism of relevant morphologies of binary FePt and CoPt nanoparticles from first principles being solely achievable on state-of-the-art supercomputer platforms.

In hard-magnetic FePt and CoPt, the energetic balance is not only influenced by the size and shape of the particle, but also by its composition and degree of chemical order. Monodisperse FePt particles with different sizes, shapes and crystal structure (A_1 and $L1_0$ phase) have been prepared by either a chemical route (e.g., [11–13]) or gas phase condensation techniques (e.g., [14,15]). Several annealing studies have shown that the transformation to the ordered $L1_0$ phase making the material interesting for ultra-high-density storage media [11] may be difficult to obtain for nm-sized particles [12,16–18] which are not embedded in a matrix or covered by organic ligands [19,20]. HRTEM investigations revealed regular, multiply twinned morphologies as icosahedra and decahedra with diameters d around 6 nm [21]. Multiple twinning is encountered if the gain in surface energy supersedes the cost of internal interfaces, such as twin boundaries [4]. The occurrence of regular, multiply twinned clusters is a consequence of the incompatibility of the faceting with the crystallographic lattice and should not be confused with the nonequilibrium twin structures observed in bulk and large particles.

By calculating the energetic state of different morphologies and crystal structures for uncontaminated (i.e., surface clean) nanoparticles, we report a first step in understanding the size, shape and environment dependent formation of the $L1_0$ state in FePt and CoPt nanoparticles from first principles. As a result we find that in clusters of to $d \approx 2.5$ nm (561 atoms) previously unreported types of chemically ordered structures are energetically favored over the $L1_0$ phase. Chemical trends are identified by means of the electronic DOS, which is also useful to distinguish the morphologies in spectroscopic measurements [22]. The calculations, which include full geometric relaxations on the Born-Oppenheimer surface, have been carried out using the Vienna *ab initio* simulation package (VASP) [23]. The valence electrons are described by a plane-wave basis set (cutoff: 268 eV, k-space sampling restricted to the Γ-point) in connection with the projector augmented wave approach [24] and the generalized gradient approximation (PW91) [25].

For binary nanoparticles, systematic *ab initio* studies are considerably more complicated than for elemental systems, since, in addition to several geometrical conformations, order-disorder and segregation tendencies have to be taken care of as well. Since a full scan of the configuration space is not practicable, we restricted our search to so-called magic cluster sizes $N = (10n^3 + 15n^2 + 11n + 3)/3 = 13, 55, 147, 309, 561$, etc., which are defined by

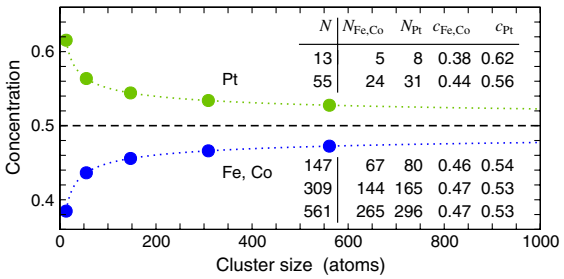

FIG. 1 (color online). Compositions of the investigated FePt and CoPt nanoclusters according to the compositions of cuboctahedra with perfect $L1_0$ order (marked by the circles).

the number n of closed geometric shells. Here, three paradigmatic geometries can be compared: Perfect cuboctahedra (single variant fcc/fct), Mackay-icosahedra [26], and Ino-decahedra [27]. We considered disordered, ordered and core-shell arrangements of the atomic species, the latter corresponding to perfect surface segregation, with all Pt placed on the surface or in the shell below. The compositions were fixed to the stoichiometric $L1_0$ ordered cuboctahedra (cf. Fig. 1), which are the most relevant isomers from the technological point of view. We focused on Pt-enriched isomers, since previous Monte Carlo simulations [28,29] and own *ab initio* results indicate that covering (001) surfaces by Pt is preferred for free $L1_0$ particles without metal-ligand interactions. Also, selected iron-rich isomers have been compared, affirming the reported trends. Perfect order in the noncrystalline structures usually implies different compositions. To avoid this, excess atoms of one species were distributed randomly over the antisites. Also, reducing the area of (001) facets in favor of (111) surfaces according to a Wulff-construction can further improve the stability of cuboctahedra and decahedra [4,30]. At present, these structures are not considered since a variety of system sizes and compositions impedes the direct comparison of the total energies and is not crucial for the identification of ordering, segregation, and chemical trends.

The evolution of the energetic order of the different FePt morphologies with the cluster size is summarized in Fig. 2. The $L1_0$ cuboctahedra (a) are chosen as energetic reference for each size and are thus located on the abscissa. The less favorable morphologies are located at positive energies, to which all disordered clusters belong, with the icosahedra (d) being more favorable than the cuboctahedra (e) and the decahedra (f). Both exhibit a tendency for reconstruction of their (001) surfaces. Ordered structures, in turn, appear in general lower in energy than $L1_0$ cuboctahedra, but well within the range of thermal energies. This applies especially to the ordered decahedra (h), where $L1_0$ order is imposed on each of the

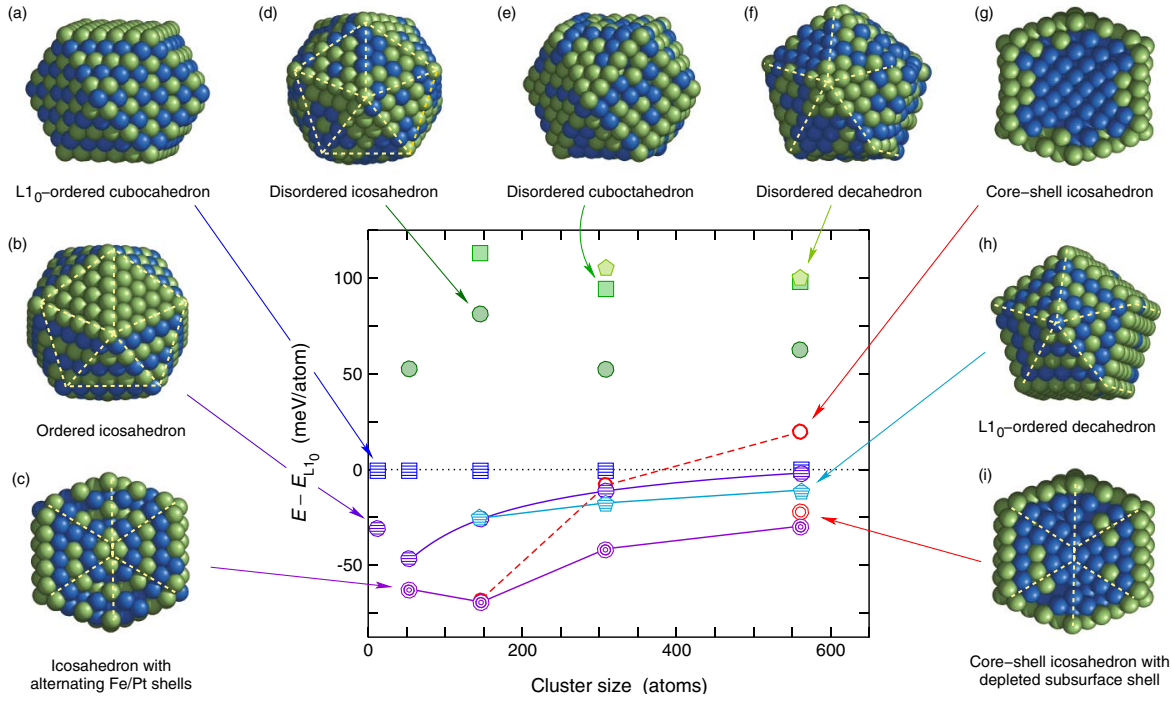

FIG. 2 (color online). Morphologies (a)–(i) of FePt nanoparticles and their corresponding energies as a function of the cluster size. The energy reference is defined by the $L1_0$ cuboctahedron (a). Only the structures with $N = 561$ atoms (265 Fe and 296 Pt) are depicted. Dark blue spheres refer to Fe atoms, bright green spheres to Pt. Some of the icosahedral structures, (c),(g) and (i), are shown as cross sections, visualizing the inner arrangement of the atomic species. The broken (yellow) lines mark the interfaces of visible twins. In the diagram, cuboctahedra are represented by squares, icosahedra by circles and decahedra by pentagons. Shaded (green) symbols denote disordered isomers, hatched (blue) symbols ordered structures, thick and nested symbols core-shell icosahedra (red) as well as icosahedra with shellwise ordering tendencies (violet). The lines are guides to the eye.

five twins individually, with the shortened c axis oriented perpendicular to the fivefold symmetry axis. The ordered icosahedron (b) evolves from the $L1_0$ structure by applying a transformation along the Mackay-path [26]. As a consequence, the two quadratic (001) surfaces of the cuboctahedron, which are entirely covered by Pt-atoms, transform to four triangular (111) facets, which no longer share the same lattice plane. This imposes distortions on the layered $L1_0$ structure which must be expected to decrease the magnetocrystalline anisotropy significantly. The ordered icosahedron is more favorable in energy for cluster sizes smaller than 561 atoms (≈ 2.5 nm). However, the diffusionless Mackay mechanism allows a transformation on much shorter time scales than diffusive ordering and segregation processes. For Lennard-Jones clusters it is known that icosahedra are supported by vibrational entropy [31], so these geometries might be found stable at finite temperatures for larger cluster sizes [10].

The most favorable morphologies are, however, icosahedra with a radially alternating arrangement of Fe and Pt shells (c), where platinum is contained only in every second shell starting with the surface shell. In icosahedra, intershell nearest neighbor distances are several percent shorter than the intrashell distances. This allows the size mismatch between the atomic species to be accommodated by a radial alternation of Fe and Pt layers and possibly reduces the internal stress in comparison to individual $L1_0$ ordering of each of the 20 twins. Core-shell structures, on the other hand, with Pt entirely segregated to the surface (g), are competitive only for $d < 2$ nm. For $N = 561$, where the number of Pt atoms exceeds the number of surface sites, the energy is by 20 meV/atom larger than that of the $L1_0$ cuboctahedron, if the excess atoms are distributed over the subsurface shell. The steep increase in energy can be traced back to the preference of the pure iron core for a bcc coordination. This results in a partial shellwise transformation along the Mackay path, as recently predicted for icosahedral Fe clusters [6]. Depletion of the subsurface shell by moving the excess Pt to the third shell (i) considerably decreases the energy by 40 meV/atom, close to the energy of (c). Isomer (i) can be regarded—in analogy to (c)—as an alternating arrangement of Pt shells with their Pt content increasing from 0% to 100% from the interior to the surface, respectively.

The DOS of small FePt particles already shares basic features of bulk $L1_0$ FePt [32], but peculiarities owing to the different morphologies exist (cf. Fig. 3). The differences are only partly due to the still important contributions of the surfaces at this size, involving 45% of the atoms. The dip in the majority channel of the icosahedron (c) at -2.25 eV, which nearly coincides with the hump in the minority channel of the $L1_0$ structure, could help to distinguish between the morphologies in spectroscopic measurements.

For CoPt, segregation is the dominant mechanism, as the comparison between the different morphologies in Fig. 4 demonstrates, where the core-shell icosahedra (g) and (i) have the lowest energies throughout the investigated size range, closely followed by the icosahedra with alternating Co and Pt shells (c). With this exception, the energetic order of the morphologies is the same as in the FePt case but appears on a different scale which is clearly exceeding the range of appropriate thermal energies (1 meV $\approx$ 11.6 K). The increased stability of the icosahedra is reflected in the DOS (Fig. 3). Since the $3d$ majority channel is practically completed, the additional d-electrons of Co fill up the states in the minority channel, shifting the contributions of the $3d$ element to lower energies in a rigid band fashion. The electron densities at the Fermi level E_{Fermi} are nearly the same for both isomers, while the minority $3d$ states of the $L1_0$ isomer encounter a considerably steeper increase above E_{Fermi}. The consequence is a larger shift of the $3d$ minority states of the multiply

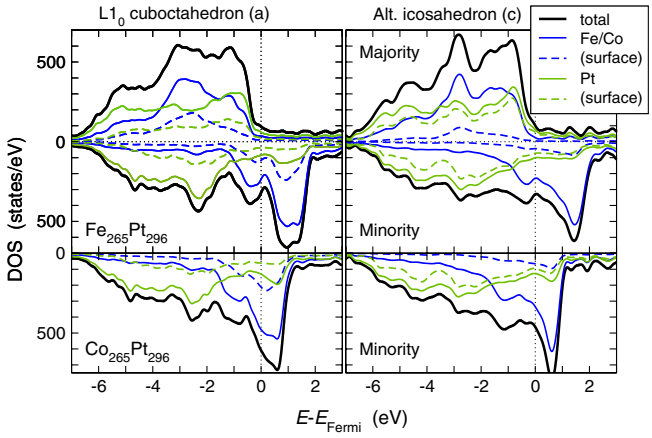

FIG. 3 (color online). Spin polarized DOS of selected $Fe_{265}Pt_{296}$ ($Co_{265}Pt_{296}$) morphologies (a) and (c) according to Fig. 2. The thick lines denote to the total DOS, the thinner lines the element-specific contributions (full lines, dark blue for Fe/Co, bright green for Pt). Dashed lines describe the contributions of the 252 surface atoms.

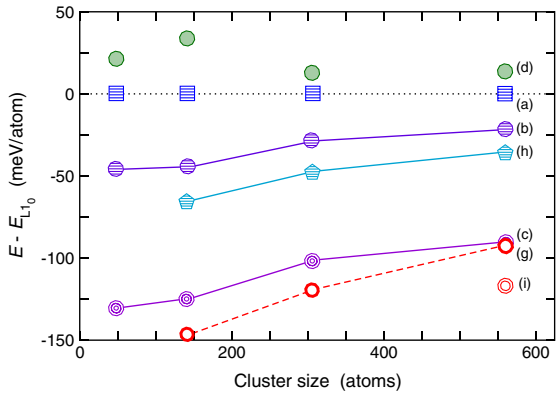

FIG. 4 (color online). Energies of CoPt clusters of various morphologies and sizes. The energy reference is again the $L1_0$ cuboctahedron. Symbols and lettering refer to the respective isomers in Fig. 2.

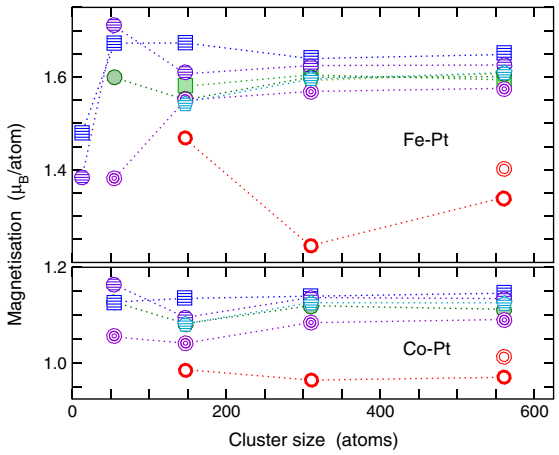

FIG. 5 (color online). Magnetization of various FePt (upper panel) and CoPt (lower panel) morphologies as a function of the cluster size. Symbols as in Fig. 2 and 4; the lines are guides to the eye.

twinned isomer, lowering its energy with respect to the $L1_0$ reference.

The magnetic properties (Fig. 5) of the ordered and disordered morphologies are very similar. The majority of the isomers are ferromagnetic with averaged spin moments of around $1.12\mu_B$/atom (CoPt) and $1.62\mu_B$/atom (FePt) for $N \geq 147$, which is in close agreement with bulk data from experiment and theory [33]. Significant deviations, however, are encountered for the core-shell isomers, (g) and (i), where the segregated Fe or Co atoms generally carry a smaller moment. In the case of FePt, the magnetization in the core is further lowered by shellwise ferrimagnetic spin arrangements. For bulk $L1_0$ FePt, competing antiferromagnetism has been predicted [34,35]. Accordingly, we found—only a few meV/atom above their ferromagnetic counterparts—antiferromagnetic $L1_0$ cuboctahedra with parallel iron layers alternating along the c axis. However, the antiferromagnetic coupling is expected to be suppressed by distortions of the $L1_0$ order [35].

Our *ab initio* DFT calculations show that the formation of multiply twinned morphologies with previously unconsidered types of chemical order are energetically favored over the $L1_0$ phase in particles of CoPt and FePt with diameters below 3 nm. From geometric considerations, it can be inferred that ordered multiply twinned morphologies will not show hard-magnetic behavior due to the different orientations of individually $L1_0$ ordered twins. This explains the recently encountered experimental difficulties to stabilize the $L1_0$ phase and to obtain the large magnetocrystalline anisotropy in uncoated FePt particles by thermal treatment [12,20,36]. We ascribe the often conflicting reports in the literature on the stabilization of the $L1_0$ phase in nonagglomerated FePt particles with a few nm in diameter to subtle changes of the electronic structure caused by oxidation of the particle surface, coverage by organic ligands or embedding in different materials. This is affirmed by structure-specific features of the electronic DOS, allowing the relative stability of specific morphologies to vary with the filling of the minority spin electronic states associated with the $3d$ element, so that it may be manipulated by chemical modification or, eventually, also by charging the particle.

The computations were performed on the Blue Gene/L supercomputer of the John von Neumann Institute for Computing (NIC) in Jülich. We thank K. Albe and O. Dmitrieva for helpful discussions. Financial support was granted by the DFG (SFB 445 and SPP 1239).

[1] I. M. L. Billas, A. Châtelain, and W. A. de Heer, Science **265**, 1682 (1994).
[2] M. L. Tiago *et al.*, Phys. Rev. Lett. **97**, 147201 (2006).
[3] F. W. Payne, W. Jiang, and L. A. Bloomfield, Phys. Rev. Lett. **97**, 193401 (2006).
[4] F. Baletto and R. Ferrando, Rev. Mod. Phys. **77**, 371 (2005).
[5] J. A. Alonso, Chem. Rev. **100**, 637 (2000).
[6] G. Rollmann *et al.*, Phys. Rev. Lett. **99**, 083402 (2007).
[7] M. A. O'Keefe *et al.*, Ultramicroscopy **89**, 215 (2001).
[8] X. Xu *et al.*, Phys. Rev. Lett. **95**, 145501 (2005).
[9] D. Sudfeld *et al.*, Mater. Res. Soc. Symp. Proc. **998**, 0998-J01-06 (2007).
[10] R. M. Wang *et al.*, Phys. Rev. Lett. **100**, 017205 (2008).
[11] S. Sun *et al.*, Science **287**, 1989 (2000).
[12] B. Stahl *et al.*, Phys. Rev. B **67**, 014422 (2003).
[13] V. Nandwana *et al.*, J. Phys. Chem. C **111**, 4185 (2007).
[14] S. Stappert *et al.*, J. Cryst. Growth **252**, 440 (2003).
[15] B. Rellinghaus *et al.*, J. Magn. Magn. Mater. **266**, 142 (2003).
[16] G. A. Held, H. Zeng, and S. Sun, J. Appl. Phys. **95**, 1481 (2004).
[17] T. Miyazaki *et al.*, Phys. Rev. B **72**, 144419 (2005).
[18] O. Dmitrieva *et al.*, J. Appl. Phys. **97**, 10N112 (2005).
[19] C. Rong *et al.*, Adv. Mater. **18**, 2984 (2006).
[20] U. Wiedwald *et al.*, Appl. Phys. Lett. **90**, 062508 (2007).
[21] Z. R. Dai, S. Sun, and Z. L. Wang, Surf. Sci. **505**, 325 (2002).
[22] H.-G. Boyen *et al.*, Adv. Mater. **17**, 574 (2005).
[23] G. Kresse and J. Furthmüller, Phys. Rev. B **54**, 11 169 (1996).
[24] G. Kresse and D. Joubert, Phys. Rev. B **59**, 1758 (1999).
[25] J. P. Perdew, in *Electronic Structure of Solids '91*, edited by P. Ziesche and H. Eschrig (Akademie Verlag, Berlin, 1991).
[26] A. L. Mackay, Acta Crystallogr. **15**, 916 (1962).
[27] S. Ino, J. Phys. Soc. Jpn. **27**, 941 (1969).
[28] M. Müller and K. Albe, Phys. Rev. B **72**, 094203 (2005).
[29] B. Yang *et al.*, Acta Mater. **54**, 4201 (2006).
[30] L. D. Marks, J. Cryst. Growth **61**, 556 (1983).
[31] J. P. K. Doye and F. Calvo, Phys. Rev. Lett. **86**, 3570 (2001).
[32] H. Ebert *et al.*, Comput. Mater. Sci. **35**, 279 (2006).
[33] A. B. Shick and O. N. Mryasov, Phys. Rev. B **67**, 172407 (2003).
[34] H. Zeng *et al.*, Phys. Rev. B **66**, 184425 (2002).
[35] G. Brown *et al.*, Phys. Rev. B **68**, 052405 (2003).
[36] C. Antoniak *et al.*, Phys. Rev. Lett. **97**, 117201 (2006).